

Geospatial Monitoring and Prediction of land Use/Land Cover (LULC) Dynamics Based on the CA-Markov Simulation Model in Ajdabiya, Libya

Aldileemi, H., Zhran, M.* and El-Mewafi, M.

Public Works Engineering Department, Faculty of Engineering, Mansoura University, Mansoura 35516, Egypt
E-mail: amgade88@gmail.com, mohamedzhran@mans.edu.eg, mmewafi1@mans.edu.eg

*Corresponding Author

DOI.ORG/ <https://doi.org/10.52939/ijg.v19i12.2973>

Abstract

The process of modelling land use and cover (LULC) is an essential tool for predicting changes in land area in the future. This study aims to define the LULC changing patterns of the Ajdabiya region in Libya for 2016, 2020, and 2022 and predict future LULC changes for 2030, 2040, and 2050 by combining Geographical Information Systems (GIS) and remote sensing with Land Change Modelling (LCM) included in the TerrSet. Sentinel satellite images were used to identify the LULC. In this study, Ajdabiya was classified into seven classes: water, urban, agricultural land, salt marsh, flat sand, sand dunes, and sand bars. The combined algorithm was used to classify the LULC classes. All the classified LULC maps demonstrate excellent accuracy, showing more than 92% overall accuracy. Implementing Cellular Automata–Markov Chain (CA-Markov) prediction model, future scenarios for LULC were developed. According to the statistics derived from the kappa indices and agreement/disagreement marks, the outcomes of predicting the LULC changes proved satisfactory. Kappa for no information (Kno) equals 0.832, Kappa for location (Klocation) equals 0.777, and Kappa for standard (Kstandard) equals 0.772. During the study period prediction from 2022 to 2050, the values of increase in the LULC classes of urban, agricultural land, salt marsh, flat sand, and sand bar are 63.69%, 43.26%, 71.03%, 35.08%, and 0.81%, respectively. By studying the LULC changing pattern, this study will assist urban planners and policymakers in choosing appropriate sustainable development options in the study area.

Keywords: Cellular Automata–Markov (CA-Markov), Land Change Modeler, Land Use/Land Cover, Libya, Modeling, Prediction, Sentinel, TerrSet

1. Introduction

The categorization of land-use/land-cover (LULC), which is frequently based on remote sensing imagery, is one of the key study topics in terms of global environmental change [1]. Investigating different changes in environmental processes and climate change at both the local and global levels require LULC information [2]. One of the most popular approaches to understanding past land usage, the types of changes calculated, the mechanisms driving such changes, and the visible changes to the Earth's surface is LULC change [3] and [4]. Critical concerns, including biodiversity destruction and detrimental effects on human existence, might be a result of LULC modifications [5] and [6]. Assessment of LULC change is now essential to many aspects of the interaction between humans and

the environment [4]. Changes in LULC are widespread and cause major concern across the world [7].

Making an accurate estimate for demand of land use and simulating it in potential future scenarios are required for land use policy and planning to be as effective as feasible [8]. Identification of LULC is essential for assessing regional, local, and global environmental change [9] and [10]. Geographic information systems (GIS) and remote sensing (RS) are effective techniques for gathering precise and current information on the spatial distribution of LULC changes. RS is an effective tool for constantly monitoring and evaluating LULC change in the environment and the development of landforms using geomorphological studies [8] and [9].



Researchers have been attracted to the cellular automata (CA) model in recent years because of its ease of use, adaptability, and capacity to integrate spatiotemporal aspects [11]. Traditional CA is insufficient to provide a realistic simulation since each individual model's structure only considers spatial data [12]. Additionally, the CA is a poor model for incorporating the dynamics that drive land use change, making it challenging to manage [8]. The Markov chain, a well-known model that predicts future change based on the past, and CA, which locates the location of change spatially [12] and [13]. The CA-Markov model was employed to attain the goals since the Markov model by itself cannot accomplish the geographical position of future LULC [14].

Numerous studies have shown that the Land Change Modeller (LCM), which is based on an integrated CA [15] and Markov chain (MC) resulting in a CA-Markov chain model, is an effective model for the study and forecasting of LULC change and urban expansion [8] [11] [16] [17] [18] and [19]. Simulating the spatiotemporal aspects of LULC dynamics is possible with the CA-Markov chain combination [14] and [20]. The combined CA-Markov model has never been used for LULC simulations in Libya. Based on Multi-Layer Perceptron neural networks (MLPNN) and CA-Markov chain, the LCM model forecasts future LULC images [21]. In this research, CA-Markov is implemented to forecast future LULC changes.

This study identified past LULC changes and simulated future changes using combined classification approach, CA-Markov, GIS spatial analysis, the ERDAS image, and the LCM. Based on the previously categorized images, the LCM integrated in TerrSet was utilized to predict the LULC in the future. For quantity estimate as well as for spatial and temporal modelling of LULC dynamics, the CA-Markov model is a reliable technique. The CA-Markov model may simulate changes in various LULCs as well as the transition from one category of LULC change to another [12] and [23]. One of the basic principles of the MC for simulating the LULC transition is that it is a stochastic process that quantifies the likelihood that one state will change to another state [12] [14] and [24]. This is made possible by the creation of a land-cover transition probability matrix (TPM), which shows that the nature of the shift may still be implemented to forecast the subsequent period [24].

Therefore, it is essential to use RS/GIS tools and simulation models to discover, identify, and model past, current, and future LULC situations. In order to create successful urban policies and plans for

economic, demographic, and environmental growth that are sustainable and maintain environmental balance, such an approach is necessary. Obtaining spatial-temporal features throughout time is a prerequisite for these strategies [14] [25] [26] and [27].

This study, which focuses on Ajdabiya in Libya, attempts to: (a) identify, quantify, and analyze in detail past LULC variations over the years 2016-2020-2022; and (b) forecast future LULC maps in the coming three decades (2030-2050) based on LCM. Additionally, this study intends to give decision-makers and policymakers a strong basis on which to build policies for sustainable development. The findings of this study might be used both within Libya and everywhere in the world. Sentinel imagery and modelling LCM will be combined to address the paper's goals. So far, to the best of our knowledge, investigating and predicting LULC in Ajdabiya have not been investigated.

2. Materials and Methods

2.1 Study Area

This study was conducted in Ajdabiya, which is the capital of the Al Wahat district in northeastern Libya. The majority of Libya is a desert nation with a dry climate and a sparse amount of vegetation. Ajdabiya is located 150 km south of Benghazi and lies along the southern side of the Mediterranean coast. Ajdabiya is located in east Libya, as presented in Figure 1. Ajdabiya is located between latitudes 27° 50' N to 31° 10' N and longitudes 18° 30' E and 21° E and has a total area of about 63900 km², as shown in Figure 1. The higher elevations were concentrated in the south, and the lower elevations were concentrated in the north. In Ajdabiya, the average annual amount of precipitation is 48 mm, and the average annual temperature is 27 °C.

2.2 Dataset

The remote sensing data employed in this study were based on Sentinel-2. Satellite images for the years 2016, 2020, and 2022 are collected by Sentinel-2, which downloaded them from the Copernicus Open Access Hub (<https://scihub.copernicus.eu/>) and then merged them into Erdas Imagine (version 15) to carry out the classifications of each LULC. High-resolution landcover monitoring is the primary objective of the Sentinel-2 satellite, which is a component of the Sentinel program. It was first launched in 2015. Sentinel-2 contains twelve spectral bands with spatial resolutions of 10, 20, and 60 m. All images were obtained in the same month for the purpose of preventing seasonal variations in the images.

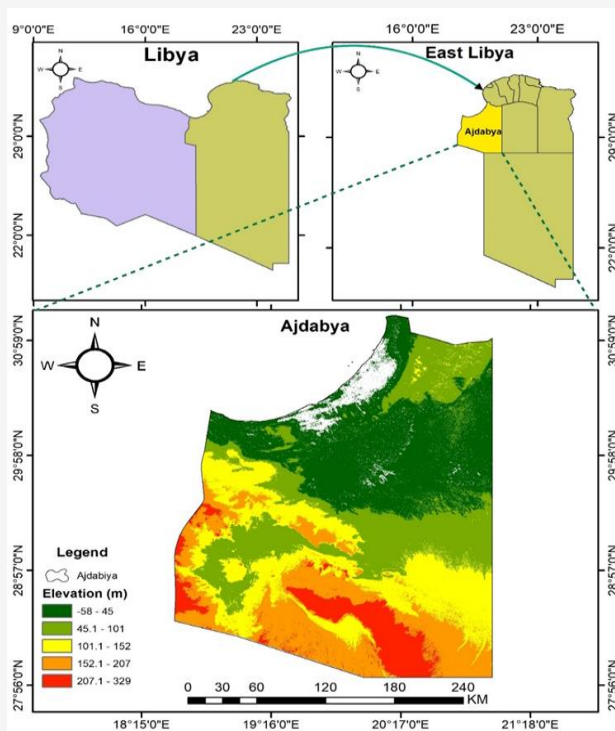


Figure 1: The study area in Ajdabiya, Libya

The whole study area is covered by sixteen images from the Sentinel-2 satellite. The Sentinel images were projected to a World Geodetic System 1984 (WGS 84) into a Universal Transverse Mercator (UTM) Zone 34 N coordinate system.

Furthermore, a 30 m digital elevation model (DEM) was extracted from the ASTER DEM (<https://www.earthdata.nasa.gov/>). Topographic features such as elevation, slope, and aspect are derived from the DEM. Road network data and hospital data are obtained from the Open Street Map (OSM) (<https://www.openstreetmap>). River data are extracted from the Global River Classification (GloRiC) (<https://www.hydrosheds.org>). The WGS 1984 UTM Zone 34 N coordinate system is applied to all the data before being input into the CA-Markov model.

2.3 Past LULC Classification and Accuracy Assessment

For the LULC classification, the combined technique was used to determine the seven main land covers using the ERDAS Imagine V. 15 software. Both manual and automatic processes are used in the combine technique. Although the combination process takes a long time, it is suited for large areas. In this study, seven classes were defined for each satellite image: water, urban, agricultural land, salt marsh, flat sand, sand dunes, and sand bar.

The selection of these classes was made according to field data and information from local people and experts. For evaluating the accuracy of the classified images, an accuracy assessment is a must. The accuracy assessment tool in Erdas was utilized, taking 98 ground truth points for the assessment of seven different LULC classes' classification accuracy. In order to evaluate the classification of the images, reference information was gathered from high-resolution imagery on Google Earth. Here, the computation of overall accuracy (OA), user accuracy (UA), producer accuracy (PA), and the kappa index of agreement served as the basis for accuracy assessment. When the kappa coefficient is less than 0.4, there is poor agreement. A value between 0.4 and 0.8 indicates moderate agreement, and a value larger than 0.8 demonstrates strong agreement, according to the authors of [20]. By dividing the total number of correctly classified pixels by the total number of reference pixels, the OA is determined [28].

2.4 Future LULC Prediction and Associated Driving Forces

Future LULC changes have been simulated using the LCM module in TerrSet software version 18.31. LCM depends on transition suitability maps produced by training multilayer perceptron or logistic regression, MC matrices, and artificial neural networks [7].

In this study, the CA-Markov model was used to forecast future LULC scenarios in Ajdabiya based on past classified images from 2016 and 2020. LCM used past LULC maps and several driving forces to map future LULC situations [3].

The selection of the input driving variables is also essential for forecasting future LULC maps [29]. The driving variables that were considered in LCM in this study are elevation, slope, aspect, distance to agriculture, distance to urban, distance to river, distance to road, and road density. The dependent and independent factors were used to predict LULC change. The driving variables are considered dependent, and LULC maps are considered independent variables. It is important to keep in mind that the choice of variables and indicators may, to some extent, result in certain variations in the simulation results or parameters of the model, which will affect the forecast of LULC change [3]. In terms of distance from the road, for instance, if the region is extremely close to the road, the rate of urbanization is quite high, and vice versa. This also holds true for other determining variables.

A stochastic modelling approach called CA-Markov model is used by the TerrSet model. The widely utilized CA-Markov model, which simulates and models the dimensions and trends of LULC evolution, was utilized to simulate future LULC scenarios [8] and [4]. The TPM and transition probability areas were created using the Markov model [22]. Assessing the possibility of LULC changing from one class to another based on area suitability transitions and the existence of driving forces is known as transition potential modelling. The TPM keeps track of the likelihood that each land use class will shift into a different class [20]. The Bayes equation, which computes the change by contrasting the first (T1) and second land cover (T2), is used by the Markov matrix model to forecast changes in land use and cover (LULC) [3] and [7]. The predicted change in pixel numbers for each LULC class throughout the designated time period is contained in the transitional area matrix. In this study, the LCM is used to predict the future LULC changes in the Ajdabiya in three scenarios (2030, 2040, and 2050) by following four steps, namely: (a) change analysis of past LULC maps (2016, 2020, and 2022); (b) constructing transition probability matrixes; (c) model validation by comparing actual and forecasted maps of the year 2022; and (d) prediction of future LULC maps for the years 2030, 2040, and 2050, taking driving forces into account [3] and [7]. The overall methodology adopted in this study is illustrated in Figure 2.

The potential for LCM in predicting future LULC was validated by creating a predicted map for 2022 based on the 2016 and 2020 LULC maps and then comparing it with the actual 2022 map. Kappa indices of agreement such as Kappa for no information (*Kno*), Kappa for location (*Klocation*), and Kappa for standard (*Kstandard*) evaluated the agreements of the two maps (actual and predicted 2022) in TerrSet [3] [8] [31] and [32]. Kappa is always less than or equal to 1. The perfect agreement between the observed and modelled data has a value of 1 [33].

Furthermore, five statistics were estimated to indicate how well the comparison map agrees with the reference map: agreement due to chance (Agreement Chance), agreement due to quantity (Agreement Quantity), agreement due to location at the grid cell level (Agreement Grid cell), disagreement due to location at the grid cell level (Disagree Grid cell), and disagreement due to quantity (Disagree Quantity) [3] [20] and [29]. To evaluate the correlations between the different driving factors, the Cramer's V Coefficient (CVC), often known as the Cramer's V method [34], was applied. CVC can assist us in identifying the degree to which a component can affect LULC change, and it ranges from 0.0 to 1.0 [29]. The CVC value is a statistical indicator of the degree of dependence or correlation between variables [20].

2.5 LULC Change Detection

Equations 1 to 3 were used to identify LULC changes based on three parameters: magnitude (degree) of change (*C*), percentage of change (*P%*), and rate of change (*R*) for each class [3] and [10].

$$C_i = L_i - B_i \quad \text{Equation 1}$$

$$P_i = \frac{C_i}{B_i} \times 100 \quad \text{Equation 2}$$

$$R_i = \frac{C_i}{T} \quad \text{Equation 3}$$

Where *i* indicates the LULC class, *B_i* and *L_i* are the areas in km² with the earliest and latter LULC, respectively. The period between *B_i* and *L_i* is *T* in years.

3. Results Analysis and Discussion

3.1 Changes in Past LULC Classes

Seven LULC classes were identified in the study area in 2016, 2020, and 2022 (Figure 3).

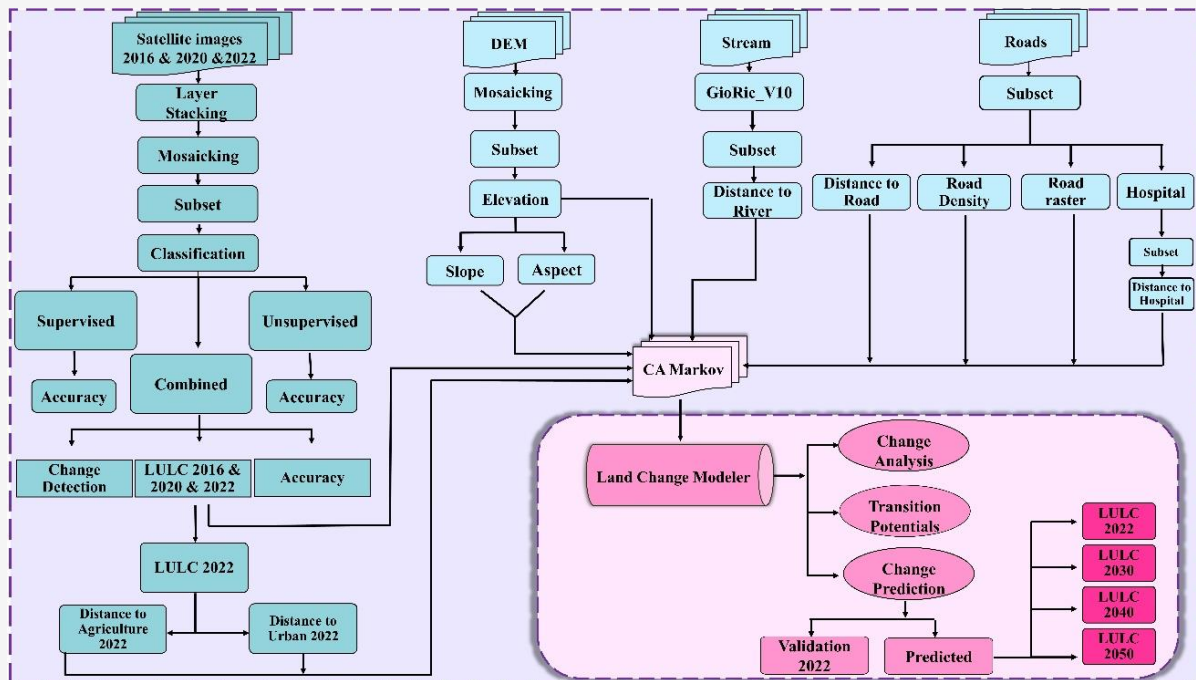


Figure 2: Methodology adopted in this study

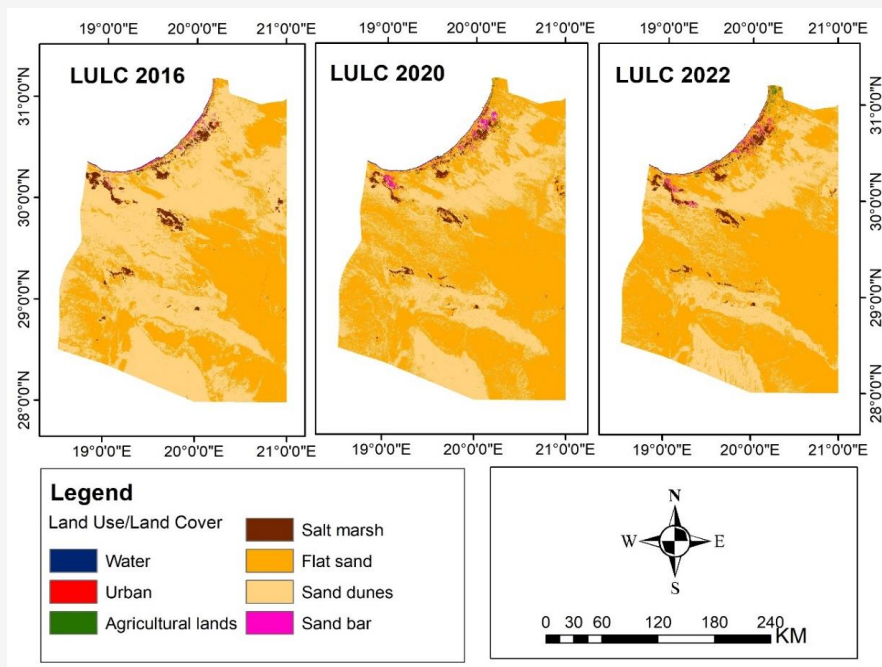


Figure 3: LULC distribution of Ajdabiya in 2016, 2020, 2022

The combined algorithm is applied to determine the LULC change patterns in 2016, 2020, and 2022, as shown in Figure 3. Table 1 provides the quantification of LULC change for the studied categories. Over the course of the research period, the largest class, which was mostly distributed over all of

Ajdabiya, was flat sand and sand dunes. As listed in Table 1, in 2016, most of the study area was covered by sand dunes (55.5%), flat sand (42%), salt marsh (1.87%), sand bars (0.33%), water (0.16%), and agricultural land (0.07%), with only a very minor part occupied by urban areas (0.05%).

Table 1: Details of LULC distribution of Ajdabiya in 2016, 2020, 2022

| LULC Type | 2016 | | 2020 | | 2022 | |
|-------------------|-------------------------|----------|-------------------------|----------|-------------------------|----------|
| | Area (km ²) | Area (%) | Area (km ²) | Area (%) | Area (km ²) | Area (%) |
| Water | 104.24 | 0.16 | 100.62 | 0.16 | 102.55 | 0.16 |
| Urban | 30.32 | 0.05 | 27.84 | 0.04 | 31.12 | 0.05 |
| Agricultural land | 42.00 | 0.07 | 70.97 | 0.11 | 183.81 | 0.29 |
| Salt marsh | 1,194.92 | 1.87 | 908.67 | 1.42 | 1,018.61 | 1.59 |
| Flat sand | 26,848.30 | 42.0 | 38,398.50 | 60.08 | 41,109.50 | 64.32 |
| Sand dunes | 35,486.10 | 55.5 | 24,078.40 | 37.67 | 21,135.10 | 33.07 |
| sand bar | 210.89 | 0.33 | 331.76 | 0.52 | 336.08 | 0.53 |
| Total | 63,916.77 | 100 | 63,916.77 | 100 | 63,916.77 | 100 |

Table 2: Accuracy of LULC classification for 2016, 2020, and 2022

| Year | Accuracy | LULC classes | | | | | | |
|------|--------------------------|--------------|-------|-------------------|------------|-----------|------------|----------|
| | | Water | Urban | Agricultural land | Salt marsh | Flat sand | Sand dunes | Sand bar |
| 2016 | PA (%) | 100 | 100 | 91.67 | 93.33 | 87.5 | 86.6 | 92.86 |
| | UA (%) | 100 | 85.71 | 78.57 | 100 | 100 | 92.86 | 92.86 |
| | OA (%) | 92.86 | | | | | | |
| | Overall Kappa statistics | 0.92 | | | | | | |
| 2020 | PA (%) | 100 | 100 | 100 | 100 | 76.47 | 81.25 | 100 |
| | UA (%) | 100 | 78.57 | 92.86 | 100 | 92.86 | 92.86 | 92.86 |
| | OA (%) | 92.86 | | | | | | |
| | Overall Kappa statistics | 0.92 | | | | | | |
| 2022 | PA (%) | 100 | 100 | 100 | 93.33 | 92.86 | 93.33 | 100 |
| | UA (%) | 100 | 85.71 | 100 | 100 | 92.86 | 100 | 100 |
| | OA (%) | 96.94 | | | | | | |
| | Overall Kappa statistics | 0.96 | | | | | | |

In 2020, there was some decrease in urban areas, and the area covered by agricultural land was 0.11%. In 2020, the urban percentage decreased compared to 2016, as mentioned in Table 1, because of the war and destruction in the study area. In 2022, the area covered by agricultural land was 0.29%, the area covered by urban areas was 0.05%, and most of the area was flat sand (64.32%). The percentage of area covered by agricultural land (0.29%) increased in 2022 compared to 2016 (0.07%). In all periods, according to the LULC maps, the percentage of flat sand increased and the percentage of sand dunes decreased. Flat sand underwent the largest increase (from 26848.30 km² in 2016 to 41109.50 km² in 2022) during the entire research period. Analysis of LULC area changes in Table 1 indicates that from 2016 to 2022, sand dunes areas decreased from 55.5% to 33.07%.

3.2 Accuracy Assessment for LULC

The final phase in the classification process was comparing the results of the combined classification with the basic actual information from PA, UA, OA,

and the Kappa accuracy statistic. To confirm the accuracy of the image classification, a confusion matrix in each LULC is constructed. The confusion matrices showed that the OA was 92.86%, 92.86%, and 96.94%, and the Kappa coefficients were 0.92, 0.92, and 0.96 for the years 2016, 2020, and 2022, respectively, as presented in Table 2. The overall kappa results of this study show a high level of data reliability. Furthermore, the analysis of the PA shows that the highest PA was obtained for the water and urban classes in all periods.

In 2020, the PA is the lowest for flat sand and sand dunes. The PA is the lowest for flat sand, sand dunes, and salt marsh in 2022. The analysis of the UA indicates that the highest UA was observed in water and salt marshes in all periods. The lowest UA was found in agricultural land (78.57%) in 2016, and the lowest PA was obtained in flat sand (76.47%) in 2020. The statistics of LULC classification accuracy were excellent, showing extremely strong agreement between the classified maps and the reference information, as can be listed in Table 2.

3.3 LULC Change Analysis and Transition Probability Matrix

Table 3 compares the three reference years: 2016, 2020, and 2022. It is possible to observe the area of LULC change, Percentage of area changing, and the rate of LULC change (R) in Ajdabiya, as listed in Table 3. The research study identified slight changes in urban areas. It can be seen from Table 3 and Figure 3 that the majority of this is flat sand and sand dunes, and over the period of 2016 to 2022, a large area of sand dunes was converted to flat sand. The positive value in percentage of change indicates an increase in a specific LULC class, while negative values indicate a decrease. The areas with the maximum increase in rate of change are flat sand and agricultural land.

Between 2016 and 2022, sand dunes' LULC classes are expected to decline by 40.44%. The decrease in salt marsh LULC classes throughout the research period (2016-2022) was 14.75%. During the study period (2016–2022), the percentage of change of increase in the LULC classes of urban, flat sand, and sand bar were 2.65%, 53.12%, and 59.40%, respectively. The results of this study showed that Ajdabiya exhibited a considerable LULC shift throughout this period of time. Table 4 demonstrates the TPM from one class to another in 2022 utilizing MC analysis for the years 2016 and 2020. The off-

diagonal data show the potential for a shift from one phenomenon to another, while the data on the diameter of TPM show the likelihood of a phenomenon remaining the same [24] and [35]. The columns of the table represent the more recent LULC categories, and the rows represent the older LULC categories.

Upon examining Table 4, it is apparent that the most important changes that occurred in the LULC simulation in 2022 are as follows: The probability to switch from water to sand bar is 0.02; from urban to flat sand is 0.27; from agricultural land to flat sand is 0.19; from salt marsh to flat sand is 0.16; from flat sand to sand dunes is 0.09; from sand dunes to flat sand is 0.34; and from sand bar to flat sand is 0.19, as revealed in Table 4. The CA-Markov model uses the TPM findings as input data to produce a simulated map of 2022. Figure 4 summarizes the "from-to" changes as LULC's loss and gain change. The investigation of gains and losses made by various categories employing change analysis in LCM showed how the LULC analysis changed, as presented in Figure 4. The study area lost 14351 km² of sand dunes (the largest loss) and gained 14261.20 km² (the largest gain) in flat sand from 2016 to 2022. Figure 4 shows that the majority of the classes have both gains and losses.

Table 3: Past LULC changes for Ajdabiya

| LULC classes | 2016-2020 | | | 2020-2022 | | | 2016-2022 | | |
|-------------------|-------------------------|----------|---------------------------|-------------------------|----------|---------------------------|-------------------------|----------|---------------------------|
| | Area (km ²) | Area (%) | R (km ² /year) | Area (km ²) | Area (%) | R (km ² /year) | Area (km ²) | Area (%) | R (km ² /year) |
| Water | -3.62 | -3.47 | -0.90 | 1.92 | 1.91 | 0.96 | -1.69 | -1.62 | -0.28 |
| Urban | -2.48 | -8.17 | -0.62 | 3.28 | 11.79 | 1.64 | 0.80 | 2.65 | 0.13 |
| Agricultural land | 28.98 | 69.00 | 7.24 | 112.84 | 158.99 | 56.42 | 141.82 | 337.68 | 23.64 |
| Salt marsh | -286.25 | -23.96 | -71.56 | 109.94 | 12.10 | 54.97 | -176.31 | -14.75 | -29.39 |
| Flat sand | 11550.2 | 43.02 | 2887.55 | 2711 | 7.06 | 1355.50 | 14261.20 | 53.12 | 2376.87 |
| Sand dunes | -11407.7 | -32.15 | -2851.93 | -2943.3 | -12.22 | -1471.65 | -14351.00 | -40.44 | -2391.83 |
| sand bar | 120.92 | 57.35 | 30.23 | 4.32 | 1.30 | 2.16 | 125.24 | 59.40 | 20.87 |

Table 4: Transition probability matrix in 2022

| Class | Water | Urban | Agricultural Land | Salt Marsh | Flat sand | Sand dunes | Sand bar |
|-------------------|--------|--------|-------------------|------------|-----------|------------|----------|
| Water | 0.9591 | 0 | 0.0036 | 0.0136 | 0.0024 | 0.0001 | 0.0211 |
| Urban | 0.0024 | 0.3357 | 0.1665 | 0.1361 | 0.2669 | 0.0693 | 0.0232 |
| Agricultural Land | 0.0118 | 0.0627 | 0.5526 | 0.1618 | 0.1881 | 0 | 0.023 |
| Salt Marsh | 0.0011 | 0.0007 | 0.0035 | 0.7696 | 0.1576 | 0.0597 | 0.0077 |
| Flat sand | 0 | 0.0003 | 0.0014 | 0.0033 | 0.8988 | 0.0943 | 0.0018 |
| Sand dunes | 0 | 0 | 0 | 0 | 0.3382 | 0.6572 | 0.0045 |
| Sand bar | 0.0006 | 0.0199 | 0.0099 | 0.0298 | 0.1915 | 0.1081 | 0.6402 |

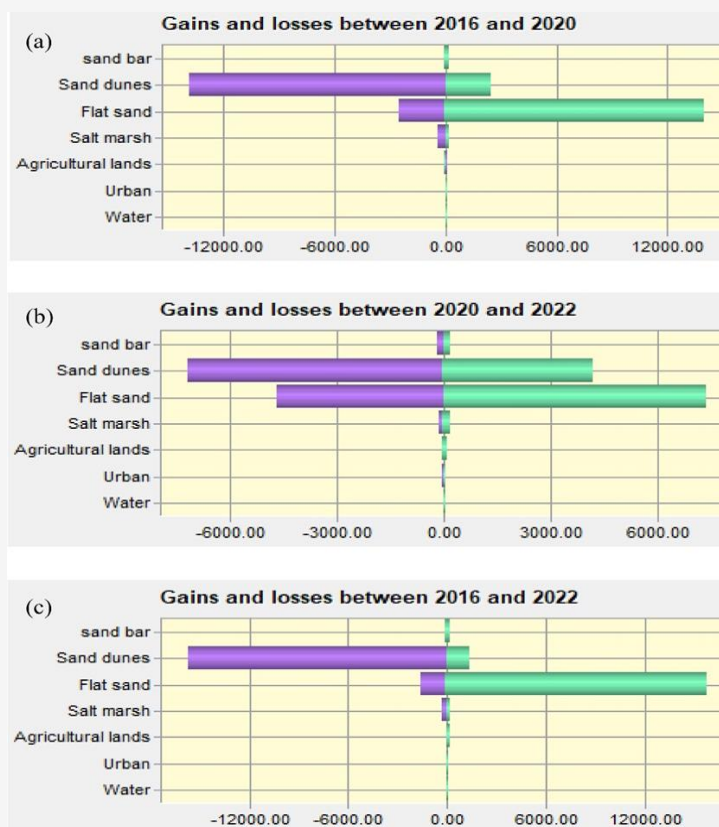


Figure 4: Gain and loss of LULC classes of the study periods: (a) from 2016 to 2020; (b) from 2020 to 2022; (c) from 2016 to 2022. The x-axis represents the area in km²

Table 5: Validation of the model accuracy for the year 2022

| Class | Area in km ² | | | | |
|-------------------|-------------------------|------------------|------------|-----------------------|--------------|
| | Actual (2022) | Predicted (2022) | Difference | Percentage difference | Accuracy (%) |
| Water | 102.55 | 101.02 | -1.53 | -1.49 | 98.51 |
| Urban | 31.12 | 30.24 | -0.88 | -2.83 | 97.17 |
| Agricultural land | 183.81 | 178.10 | -5.71 | -3.11 | 96.89 |
| Salt marsh | 1,018.61 | 1,041.85 | 23.24 | 2.28 | 97.72 |
| Flat sand | 41,109.50 | 41,495.40 | 385.90 | 0.94 | 99.06 |
| Sand dunes | 21,135.10 | 20,748.40 | -386.70 | -1.83 | 98.17 |
| sand bar | 336.08 | 321.84 | -14.24 | -4.24 | 95.76 |

3.4 Model Validation

The purpose of the validation process was to evaluate the predicted map. The LULC map of 2022, predicted from the 2016 and 2020 data, has been validated with the classified LULC map of the same year (Table 5), demonstrating how well the LCM model can effectively predict LULC changes with an average accuracy of 97.61%. Table 5 lists the prediction model accuracy, which varied between 95.76% and 99.06%, with an average accuracy of about 97.61% for different LULC. Kappa indices and other statistics in TerrSet were used to evaluate LCM's potential to forecast the 2022 LULC, as compiled in

Table 6. *Klocation* equals 0.777 and *Kstandard* equals 0.772, as listed in Table 6. All the calculated *K-index* values (>75%) show good agreement between the predicted and actual LULC maps. For evaluating the simulation's accuracy, *Kno* is the most crucial parameter. As observed in Table 6, *Kno* equals 0.8315, which means that the CA-Markov model has the ability for future prediction with sufficient accuracy. As far as the authors are aware, the performance of the CA-Markov in LCM for the LULC pattern has never been evaluated in this study area.

Table 6: Statistical verification of the CA-Markov model for predicting LULC in 2022

| Statistics | Value |
|------------------------|--------|
| <i>Kno</i> | 0.8315 |
| <i>Klocation</i> | 0.7773 |
| <i>Kstandard</i> | 0.7716 |
| Agreement Chance | 0.1250 |
| Agreement Quantity | 0.2296 |
| Agreement Grid cell | 0.4980 |
| Disagreement Grid cell | 0.1427 |
| Disagreement Quantity | 0.0047 |

Table 7: Cramer's V coefficients of driving forces

| Driving Force | Cramer's V Value |
|-------------------------|------------------|
| Distance to Agriculture | 0.0714 |
| Distance to Urban | 0.1022 |
| Elevation | 0.1609 |
| Aspect | 0.0626 |
| Slope | 0.0506 |
| Distance to River | 0.0871 |
| Distance to Road | 0.0586 |
| Road Density | 0.1347 |
| Distance to Hospital | 0.1493 |

Table 8: Transition probability matrix in 2030

| Class | Water | Urban | Agricultural Land | Salt Marsh | Flat sand | Sand dunes | Sand bar |
|-------------------|-------|-------|-------------------|------------|-----------|------------|----------|
| Water | 0.81 | 0.00 | 0.01 | 0.04 | 0.07 | 0.02 | 0.05 |
| Urban | 0.01 | 0.02 | 0.06 | 0.14 | 0.59 | 0.16 | 0.02 |
| Agricultural Land | 0.02 | 0.02 | 0.09 | 0.19 | 0.53 | 0.12 | 0.03 |
| Salt Marsh | 0.00 | 0.00 | 0.01 | 0.30 | 0.52 | 0.16 | 0.01 |
| Flat sand | 0.00 | 0.00 | 0.00 | 0.01 | 0.78 | 0.20 | 0.01 |
| Sand dunes | 0.00 | 0.00 | 0.00 | 0.01 | 0.70 | 0.28 | 0.01 |
| Sand bar | 0.00 | 0.01 | 0.01 | 0.05 | 0.58 | 0.20 | 0.14 |

The LULC change maps for later dates were predicted when the LULC map for 2022 was correctly forecast. In particular, the disagreement grid cell and disagreement quantity parameters are essential when evaluating the model's simulated outcomes [29]. According to the findings in Table 6, the disagree grid cell is larger than the disagree quantity. This indicates that the model can better forecast changes in the study area's LULC quantity than its location.

3.5 Future LULC Simulations for 2030, 2040 and 2050

To predict future LULC changes, it is required to consider the most crucial driving forces listed in Table 7. The table summarizes the Cramer's V coefficients of driving forces. The decision whether to accept or reject a driver variable was based on Cramer's V values [23]. Very low Cramer's V variables can be removed from the model.

A high value is seen as beneficial (often larger than 0.1) [23]. Here, all Cramer's V for the nine-driving factor is greater than or equal 0.1 after the approximation. LCM uses past LULC maps and several driving variables (Figure 5) to map potential LULC scenarios in the future, as illustrated in Figure 6. The maps presented in Figure 5 were used as input in TerrSet. The future LULC predictions for 2030, 2040, and 2050 in Ajdabiya were obtained, followed by the same method used for the prediction of LULC for 2022 via LCM, as highlighted in Figure 6. Table 8 demonstrates the TPM from one class to another in 2030. Table 8 shows the most important changes that occurred in the LULC simulation in 2030. The CA-Markov model uses the TPM results as input data to produce a predicted map for 2030. This study provides a better understanding of LULC changes for better resource management and decision-making. Tables 9 and 10 present the TPM from one class to another in 2040 and 2050, respectively.

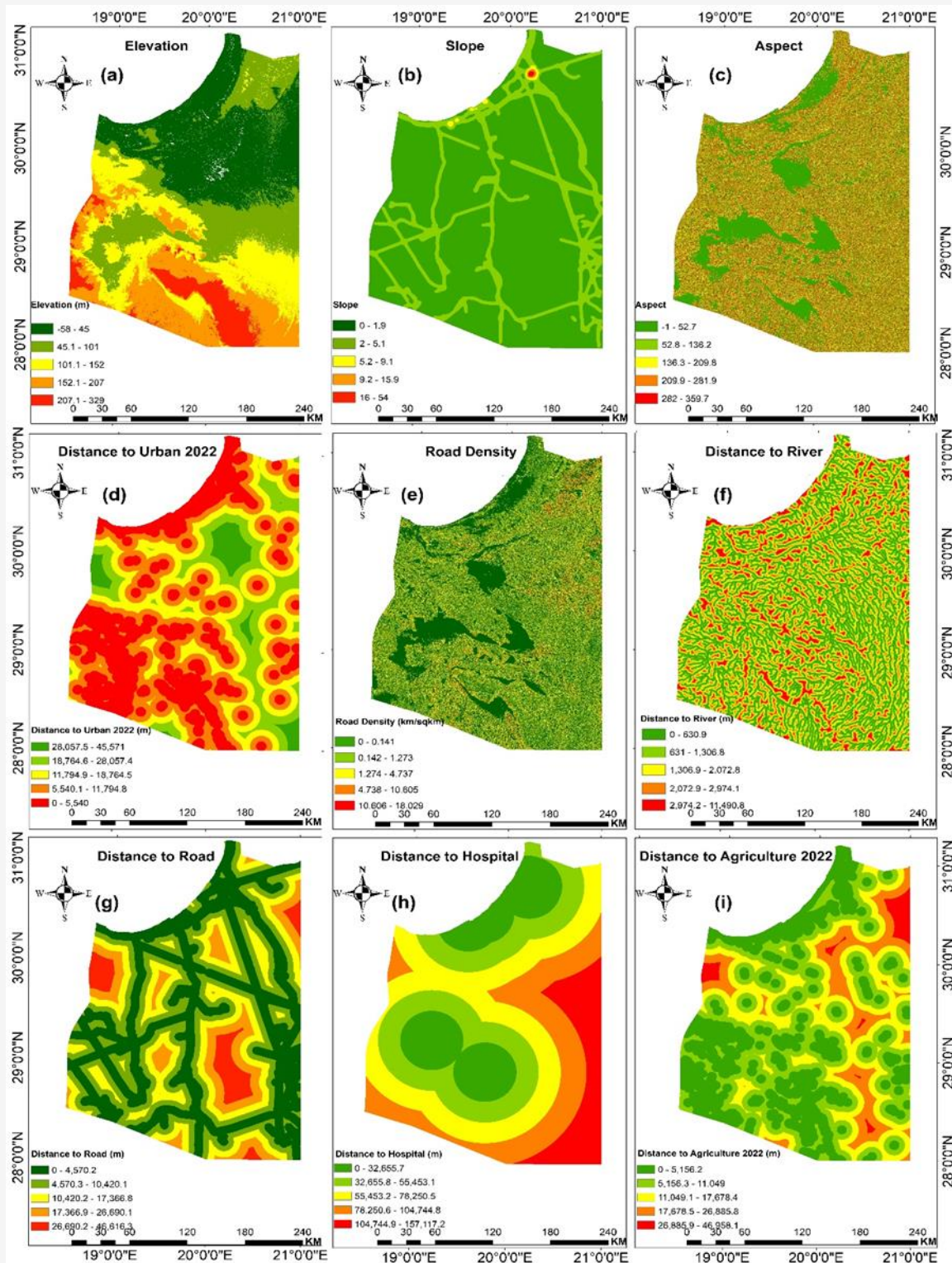


Figure 5: Driving variables used in the LCM simulations: (a) elevation (b) slope (c) aspect (d) distance to urban (e) road density (f) distance to river (g) distance to road (h) distance to hospital (i) distance to agriculture

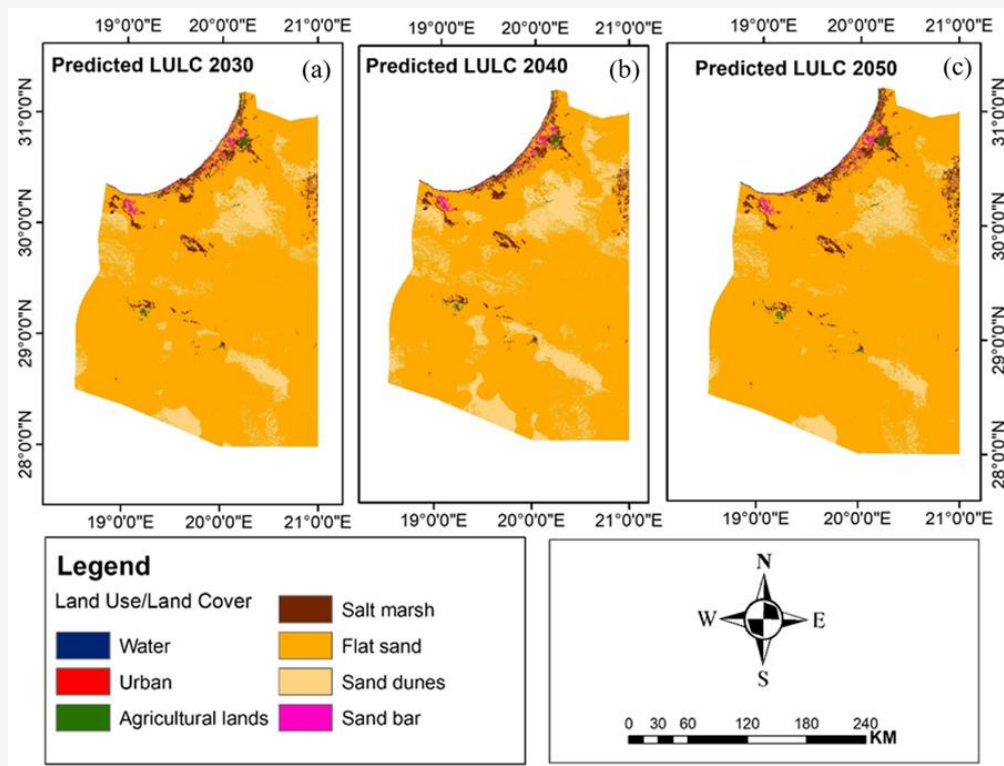


Figure 6: LULC prediction maps for (a) 2030 (b) 2040 (c) 2050

Table 9: Transition probability matrix in 2040

| Class | Water | Urban | Agricultural Land | Salt Marsh | Flat sand | Sand dunes | Sand bar |
|-------------------|-------|-------|-------------------|------------|-----------|------------|----------|
| Water | 0.66 | 0.00 | 0.01 | 0.05 | 0.18 | 0.05 | 0.05 |
| Urban | 0.01 | 0.00 | 0.01 | 0.07 | 0.70 | 0.20 | 0.01 |
| Agricultural Land | 0.02 | 0.00 | 0.02 | 0.09 | 0.67 | 0.19 | 0.01 |
| Salt Marsh | 0.00 | 0.00 | 0.00 | 0.10 | 0.68 | 0.20 | 0.01 |
| Flat sand | 0.00 | 0.00 | 0.00 | 0.01 | 0.75 | 0.22 | 0.01 |
| Sand dunes | 0.00 | 0.00 | 0.00 | 0.01 | 0.76 | 0.22 | 0.01 |
| Sand bar | 0.00 | 0.00 | 0.01 | 0.03 | 0.71 | 0.21 | 0.03 |

Table 10: Transition probability matrix in 2050

| Class | Water | Urban | Agricultural Land | Salt Marsh | Flat sand | Sand dunes | Sand bar |
|-------------------|-------|-------|-------------------|------------|-----------|------------|----------|
| Water | 0.54 | 0.00 | 0.01 | 0.05 | 0.28 | 0.08 | 0.04 |
| Urban | 0.01 | 0.00 | 0.00 | 0.03 | 0.74 | 0.21 | 0.01 |
| Agricultural Land | 0.02 | 0.00 | 0.00 | 0.04 | 0.72 | 0.20 | 0.01 |
| Salt Marsh | 0.00 | 0.00 | 0.00 | 0.04 | 0.73 | 0.21 | 0.01 |
| Flat sand | 0.00 | 0.00 | 0.00 | 0.01 | 0.76 | 0.21 | 0.01 |
| Sand dunes | 0.00 | 0.00 | 0.00 | 0.01 | 0.76 | 0.21 | 0.01 |
| Sand bar | 0.00 | 0.00 | 0.00 | 0.02 | 0.75 | 0.21 | 0.01 |

Remarkably, during the previous two decades, the likelihood of turning urban land into agricultural land fell dramatically, from 1.06 to 0.4%. The value of the future LULC change and the annual rate of change of LULC classes for Ajdabiya were estimated to illustrate the changes of the LULC classes in different

periods, as highlighted in Table 11. The value of the decrease in the LULC classes of sand dunes between 2040 and 2050 is 49.22%. During the study period (2022–2050), the decrease in the LULC classes of sand dunes was 74.20%.

Table 11: Future LULC changes for Ajdabiya

| LULC classes | 2022-2030 | | 2030-2040 | | 2040-2050 | | 2022-2050 | |
|-------------------|-------------------------|----------|-------------------------|----------|-------------------------|----------|-------------------------|----------|
| | Area (km ²) | Area (%) |
| Water | 0.00 | 0.00 | 0.00 | 0.00 | 0.00 | 0.00 | 0.00 | 0.00 |
| Urban | 12.04 | 39.81 | 0.03 | 0.00 | 7.19 | 17.00 | 19.26 | 63.69 |
| Agricultural land | 42.21 | 23.70 | -15.16 | -0.07 | 50.00 | 24.37 | 77.05 | 43.26 |
| Salt marsh | 422.43 | 40.55 | 38.08 | 0.03 | 279.49 | 18.60 | 740.00 | 71.03 |
| Flat sand | 13,298.40 | 32.05 | -3,589.20 | -0.07 | 4,847.60 | 9.47 | 14,556.80 | 35.08 |
| Sand dunes | -13,768.07 | -66.36 | 3,560.47 | 0.51 | -5,188.17 | -49.22 | -15,395.77 | -74.20 |
| sand bar | -7.07 | -2.20 | 5.71 | 0.02 | 3.97 | 1.24 | 2.62 | 0.81 |

During the study period (2022–2050), the values of increase in the LULC classes of urban, agricultural land, salt marsh, flat sand, and sand bar were 63.69%, 43.26%, 71.03%, 35.08%, and 0.81%, respectively. The findings of this study indicated that there was a significant LULC change in Ajdabiya during this period. The distribution of flat sand and sand dunes in the research region has been impacted by variations in LULC. The greatest portion of the LULC class, the flat sand region, has grown greatly, while the second-largest portion, the sand dunes area, has shrunk dramatically. Similarly, urban areas and agricultural lands increased from 2022 to 2050. The combined CA-Markov model using Sentinel satellite imagery effectively provides a better understanding of changes in LULC. As a result, the drivers of LULC dynamics were used in this study to analyze the LULC dynamics of the past and future LULC using Sentinel images and LCM. As a result, this research will also aid in evaluating the effectiveness of the CA-Markov strategy in the Ajdabiya region.

4. Conclusions

This study used Sentinel satellite images to identify and simulate the LULC changes in Ajdabiya, Libya. The goal of the current study was to investigate how past and predicted land use and land cover patterns will change between 2016 and 2050, with an emphasis on water, urban, agricultural land, salt marsh, flat sand, sand dunes, and sand bars. The multitemporal Sentinel satellite imaging data are utilized to support informed LULC change decision-making by potentially supplying the data needed for LULC change monitoring and evaluation. The images are classified based on the combine method. All the classified LULC maps show excellent accuracy, showing more than 92% overall accuracy. To comprehend the spatiotemporal nature of LULC dynamics and forecast future LULC change, an integrated approach combining remote sensing, GIS, and a CA-Markov model was utilized. The LCM was

implemented to predict LULC over the next three decades (years 2030, 2040, and 2050). By comparing the expected scenario with the actual one acquired from satellite images, the 2022 LULC map was utilized to validate the LCM technique, demonstrating that the employed CA-Markov has the capability to predict future LULC. The LULC maps for 2030, 2040, and 2050 are forecast following successful model validation. For modelling LULC change, combining the Markov model with CA is expected to produce predictions that are most accurate when utilizing the transition probability matrix.

By estimating the Ajdabiya LULC for the ensuing three decades (2030, 2040, and 2050) based on past data (LULC in 2016, 2020, and 2022), the current work seeks to fill this gap and infer patterns that may be used in a variety of scenarios. However, Ajdabiya has not conducted similar research; therefore, this work is very significant. Sand dunes cover has been declining, while flat sand, salt marsh, urban, and agricultural areas are all rising rapidly, according to the analysis of LULC change from 2022 to 2050. According to this analysis, the sand dunes area, which makes up the second-biggest component of the LULC class, has drastically diminished, while the flat sand region, which makes up the largest amount, has expanded significantly from 2022 to 2050.

As a result, in order to facilitate sustainable growth, policymakers must adopt appropriate and timely management measures. The methods and results of this study will be beneficial for the concerned authorities, government representatives, policymakers, and urban planners who can use the findings for thorough area planning to make the Ajdabiya livable by planting trees, conserving water bodies, and planning urban infrastructural development to make the Ajdabiya planned and environmentally sustainable. Additionally, this type of study has a strong potential to support regional and local sustainable development.

References

- [1] Guan, D. J., Li, H. F., Inohae, T., Su, W., Nagaie, T. and Hokao, K., (2011). Modeling Urban Land Use Change by the Integration of Cellular Automaton and Markov Model. *Ecol Modell*, Vol. 222, 3761–3772, <https://doi.org/10.1016/j.ecolmodel.2011.09.009>.
- [2] Das, N., Mondal, P., Sutradhar, S. and Ghosh, R., (2021). Assessment of Variation of Land Use/Land Cover and Its Impact on Land Surface Temperature of Asansol Subdivision. *Egyptian Journal of Remote Sensing and Space Science*, Vol. 24, 131–149, <https://doi.org/10.1016/j.ejrs.2020.05.001>.
- [3] Regasa, M.S. and Nones, M., (2022). Past and Future Land Use/Land Cover Changes in the Ethiopian Fincha Sub-Basin. *Land (Basel)*, Vol. 11(8), 1-20. <https://doi.org/10.3390/land11081239>.
- [4] Alam, A., Bhat, M. S. and Maheen, M., (2020). Using Landsat Satellite Data for Assessing the Land Use and Land Cover Change in Kashmir Valley. *GeoJournal*, Vol. 85, 1529–1543, <https://doi.org/10.1007/s10708-019-10037-x>.
- [5] Leta, M. K., Demissie, T. A. and Tränckner, J., (2021). Hydrological Responses of Watershed to Historical and Future Land Use Land Cover Change Dynamics of Nashe Watershed, Ethiopia. *Water (Switzerland)*, Vol. 13, 1-20, <https://doi.org/10.3390/w13172372>.
- [6] Khan, T. U., Mannan, A., Hacker, C. E., Ahmad, S., Siddique, M. A., Khan, B. U., Din, E. U., Chen, M., Zhang, C., Nizami, M. and Luan, X., (2021). Use of GIS and Remote Sensing Data to Understand the Impacts of Land Use/Land Cover Changes (Lulcc) on Snow Leopard (*Panthera Uncia*) Habitat in Pakistan. *Sustainability (Switzerland)*, Vol. 13(7), 1-19. <https://doi.org/10.3390/su13073590>.
- [7] Hasan, S., Shi, W., Zhu, X., Abbas, S. and Khan, H. U. A., (2020). Future Simulation of Land Use Changes in Rapidly Urbanizing South China Based on Land Change Modeler and Remote Sensing Data. *Sustainability (Switzerland)*, Vol. 12(11), 1-24. <https://doi.org/10.3390/su12114350>.
- [8] Beroho, M., Briak, H., Cherif, E. K., Boulahfa, I., Ouallali, A., Mrabet, R., Kebede, F., Bernardino, A. and Aboumaria, K., (2023). Future Scenarios of Land Use/Land Cover (LULC) Based on a CA-Markov Simulation Model: Case of a Mediterranean Watershed in Morocco. *Remote Sens (Basel)*, Vol. 15, <https://doi.org/10.3390/rs15041162>.
- [9] Seyam, M. M. H., Haque, M. R. and Rahman, M. M., (2023). Identifying the Land Use Land Cover (LULC) Changes Using Remote Sensing and GIS Approach: A Case Study at Bhaluka in Mymensingh, Bangladesh. *Case Studies in Chemical and Environmental Engineering*, Vol. 7(10), 1-12. <https://doi.org/10.1016/j.cscee.2022.100293>.
- [10] Vivekananda, G. N., Swathi, R. and Sujith, A. V. L. N., (2001). Multi-Temporal Image Analysis for LULC Classification and Change Detection. *Eur. J. Remote Sens.*, Vol. 54, 189–199, <https://doi.org/10.1080/22797254.2020.1771215>.
- [11] Abdelkarim, A., (2023). Monitoring and Forecasting of Land Use/Land Cover (LULC) in Al-Hassa Oasis, Saudi Arabia Based on the Integration of the Cellular Automata (CA) and the Cellular Automata-Markov Model (CA-Markov). *Geology, Ecology, and Landscapes*, 1-32, <https://doi.org/10.1080/24749508.2022.2163741>.
- [12] Arsanjani, J. J., Helbich, M., Kainz, W. and Bolorani, A. D., (2013). Integration of Logistic Regression, Markov Chain and Cellular Automata Models to Simulate Urban Expansion. *International Journal of Applied Earth Observation and Geoinformation*, Vol. 21, 265–275, <https://doi.org/10.1016/j.jag.2011.12.014>.
- [13] Rimal, B., Zhang, L., Keshtkar, H., Haack, B. N., Rijal, S. and Zhang, P., (2018). Land Use/Land Cover Dynamics and Modeling of Urban Land Expansion by the Integration of Cellular Automata and Markov Chain. *ISPRS International Journal of Geo-Information*, Vol. 7(4), <https://doi.org/10.3390/ijgi7040154>.
- [14] Rimal, B., Zhang, L., Keshtkar, H., Wang, N. and Lin, Y., (2017). Monitoring and Modeling of Spatiotemporal Urban Expansion and Land-Use/Land-Cover Change Using Integrated Markov Chain Cellular Automata Model. *ISPRS International Journal of Geo-Information*, Vol. 6(9), 1-21. <https://doi.org/10.3390/ijgi6090288>.

- [15] Araya, Y. H. and Cabral, P., (2010). Analysis and Modeling of Urban Land Cover Change in Setúbal and Sesimbra, Portugal. *Remote Sens (Basel)*, Vol. 2, 1549–1563, <https://doi.org/10.3390/rs2061549>.
- [16] Megahed, Y., Cabral, P., Silva, J. and Caetano, M., (2015). Land Cover Mapping Analysis and Urban Growth Modelling Using Remote Sensing Techniques in Greater Cairo Region-Egypt. *ISPRS International Journal of Geo-Information*, Vol. 4, 1750–1769, <https://doi.org/10.3390/ijgi4031750>.
- [17] Mishra, V., Rai, P. and Mohan, K., (2014). Prediction of Land Use Changes Based on Land Change Modeler (LCM) Using Remote Sensing: A Case Study of Muzaffarpur (Bihar), India. *Journal of the Geographical Institute Jovan Cvijic*, Vol. 64, 111–127, <https://doi.org/10.2298/ijgi1401111m>.
- [18] Ozturk, D., (2015). Urban Growth Simulation of Atakum (Samsun, Turkey) Using Cellular Automata-Markov Chain and Multi-Layer Perceptron-Markov Chain Models. *Remote Sens (Basel)*, Vol. 7, 5918–5950, <https://doi.org/10.3390/rs70505918>.
- [19] Kulithalai Shiyam Sundar, P. and Deka, P. C., (2022). Spatio-Temporal Classification and Prediction of Land Use and Land Cover Change for the Vembanad Lake System, Kerala: A Machine Learning Approach. *Environmental Science and Pollution Research*, Vol. 29, 86220–86236.
- [20] Leta, M. K., Demissie, T. A. and Tränckner, J., (2021). Modeling and Prediction of Land Use Land Cover Change Dynamics Based on Land Change Modeler (Lcm) in Nashe Watershed, Upper Blue Nile Basin, Ethiopia. *Sustainability (Switzerland)*, Vol. 13, <https://doi.org/10.3390/su13073740>.
- [21] Wu, Q., Li, H. Q., Wang, R. S., Paulussen, J., He, Y., Wang, M., Wang, B. H. and Wang, Z., (2006). Monitoring and Predicting Land Use Change in Beijing Using Remote Sensing and GIS. *Landsc Urban Plan*, Vol. 78, 322–333, <https://doi.org/10.1016/j.landurbplan.2005.10.002>.
- [22] Nath, B., Wang, Z., Ge, Y., Islam, K., Singh, R. P. and Niu, Z., (2020) Land Use and Land Cover Change Modeling and Future Potential Landscape Risk Assessment Using Markov-CA Model and Analytical Hierarchy Process. *ISPRS Int J Geoinf*, Vol. 9, <https://doi.org/10.3390/ijgi9020134>.
- [23] Islam, K., Rahman, M. F. and Jashimuddin, M., (2018). Modeling Land Use Change Using Cellular Automata and Artificial Neural Network: The Case of Chunati Wildlife Sanctuary, Bangladesh. *Ecol Indic*, Vol. 88, 439–453, <https://doi.org/10.1016/j.ecolind.2018.01.047>.
- [24] Keshtkar, H. and Voigt, W., (2016). A Spatiotemporal Analysis of Landscape Change Using an Integrated Markov Chain and Cellular Automata Models. *Model Earth Syst Environ*, Vol. 2(1), <https://doi.org/10.1007/s40808-015-0068-4>.
- [25] Shafizadeh Moghadam, H. and Helbich, M., (2013). Spatiotemporal Urbanization Processes in the Megacity of Mumbai, India: A Markov Chains-Cellular Automata Urban Growth Model. *Applied Geography*, Vol. 40, 140–149, <https://doi.org/10.1016/j.apgeog.2013.01.009>.
- [26] Weng, Q., (2002). Land Use Change Analysis in the Zhujiang Delta of China Using Satellite Remote Sensing, GIS and Stochastic Modelling. *J Environ Manage*, Vol. 64, 273–284, <https://doi.org/10.1006/jema.2001.0509>.
- [27] Feng, Y., Lu, D., Moran, E. F., Dutra, L. V., Calvi, M. F. and de Oliveira, M. A. F., (2017). Examining Spatial Distribution and Dynamic Change of Urban Land Covers in the Brazilian Amazon Using Multitemporal Multisensor High Spatial Resolution Satellite Imagery. *Remote Sens (Basel)*, Vol. 9, <https://doi.org/10.3390/rs9040381>.
- [28] Mishra, V. N. and Rai, P.K., (2016). A Remote Sensing Aided Multi-Layer Perceptron-Markov Chain Analysis for Land Use and Land Cover Change Prediction in Patna District (Bihar), India. *Arabian Journal of Geosciences*, Vol. 9, <https://doi.org/10.1007/s12517-015-2138-3>.
- [29] Wang, W., Zhang, C., Allen, J. M., Li, W., Boyer, M. A., Segerson, K. and Silander, J. A., (2016). Analysis and Prediction of Land Use Changes Related to Invasive Species and Major Driving Forces in the State of Connecticut. *Land (Basel)*, Vol. 5, <https://doi.org/10.3390/land5030025>.
- [30] de Oliveira Barros, K., Alvares Soares Ribeiro, C. A., Marcatti, G. E., Lorenzon, A. S., Martins de Castro, N. L., Domingues, G. F., Romário de Carvalho, J. and Rosa dos Santos, A., (2018). Markov Chains and Cellular Automata to Predict Environments Subject to Desertification. *J Environ Manage*, Vol. 225, 160–167, <https://doi.org/10.1016/j.jenvman.2018.07.064>.

- [31] Dey, N. N., Al Rakib, A., Kafy, A. Al. and Raikwar, V., (2021). Geospatial Modelling of Changes in Land Use/Land Cover Dynamics Using Multi-Layer Perception Markov Chain Model in Rajshahi City, Bangladesh. *Environmental Challenges*, Vol. 4, <https://doi.org/10.1016/j.envc.2021.100148>.
- [32] Wang, J.; Maduako, I.N., (2018). Spatio-Temporal Urban Growth Dynamics of Lagos Metropolitan Region of Nigeria Based on Hybrid Methods for LULC Modeling and Prediction. *Eur J Remote Sens*, Vol. 51, 251–265, <https://doi.org/10.1080/22797254.2017.1419831>.
- [33] Sari, I. L., Weston, C. J., Newnham, G. J. and Volkova, L., (2023). Land Cover Modelling for Tropical Forest Vulnerability Prediction in Kalimantan, Indonesia. *Remote Sens Appl*, Vol. 32, <https://doi.org/10.1016/j.rsase.2023.101003>.
- [34] David, F. N., Cramer, H. and Cramer, H., (2016). *Mathematical Methods of Statistics (PMS-9)*. Princeton University Press: Princeton, NJ, USA, Volume 9, <https://doi.org/10.2307/2332454>.
- [35] Guan, D. J., Li, H. F., Inohae, T., Su, W., Nagaie, T. and Hokao, K., (2011). Modeling Urban Land Use Change by the Integration of Cellular Automaton and Markov Model. *Ecol Modell*, Vol. 222, 3761–3772, <https://doi.org/10.1016/j.ecolmodel.2011.09.009>.